

Scalable Multi-Modal Multi-Objective Test Problems with Respect to Decision Space Dimensionality and Pareto Set Dimensionality: High-Dimensional Manhattan Distance Minimization Problems

Hisao Ishibuchi[†]

Southern University of Science
and Technology
Shenzhen, China
hisao@sustech.edu.cn

Tianye Shu

Southern University of Science
and Technology
Shenzhen, China
12431261@mail.sustech.edu.cn

Lie Meng Pang

Southern University of Science
and Technology
Shenzhen, China
panglm@sustech.edu.cn

ABSTRACT

In most multi-objective test problems, the dimensionality of the Pareto set is the same as the dimensionality of the Pareto front. That is, an m -objective test problem with n decision variables usually has an $(m-1)$ -dimensional Pareto front and an $(m-1)$ -dimensional Pareto set. Thanks to this property, the mapping between the Pareto front and the Pareto set is usually a one-to-one mapping. In this paper, we formulate two-objective distance minimization problems in an n -dimensional decision space using Manhattan distance. The two objectives are defined by two target points in the decision space. That is, each objective is to minimize the Manhattan distance from the solution to each target point. The main characteristic feature of our test problems is that the dimensionality of the Pareto set can be arbitrarily specified between 1 and n by the locations of the two target points. For example, the Pareto set dimensionality in a 20-dimensional decision space is an arbitrarily specified integer between 1 and 20. These test problems have multimodality since many points in the Pareto set are mapped to the same single point on the Pareto front. In this paper, we first explain the relation between the locations of the two target points and the Pareto set dimensionality. Then, through computational experiments, we show that our simple test problems pose difficult challenges for both multi-objective algorithms and multi-modal multi-objective algorithms. We also discuss the scalability of the proposed test problems with respect to the number of equivalent Pareto sets and the number of objectives.

CCS CONCEPTS

Mathematics of computing → Evolutionary algorithms.

[†]Corresponding Author

Permission to make digital or hard copies of all or part of this work for personal or classroom use is granted without fee provided that copies are not made or distributed for profit or commercial advantage and that copies bear this notice and the full citation on the first page. Copyrights for components of this work owned by others than the author(s) must be honored. Abstracting with credit is permitted. To copy otherwise, or republish, to post on servers or to redistribute to lists, requires prior specific permission and/or a fee. Request permissions from Permissions@acm.org. *FOGA '25, August 27–29, 2025, Leiden, Netherlands*

© 2025 Copyright is held by the owner/author(s). Publication rights licensed to ACM. ACM ISBN 979-8-4007-1859-5/25/08
<https://doi.org/10.1145/3729878.3746701>

KEYWORDS

Evolutionary multi-objective optimization (EMO), Multi-modal multi-objective optimization, distance minimization problems, high-dimensional Pareto sets, Manhattan distance.

ACM Reference format:

Hisao Ishibuchi, Tianye Shu and Lie Meng Pang. 2025. Scalable Multi-Modal Multi-Objective Test Problems with Respect to Decision Space Dimensionality and Pareto Set Dimensionality: High-Dimensional Manhattan Distance Minimization Problems. In *Proceedings of Conference on Foundations of Genetic Algorithms (FOGA '25) Aug 27-29, 2025, Leiden, The Netherlands*. ACM, New York, NY, USA, 12 pages. <https://doi.org/10.1145/3729878.3746701>

1 Introduction

In the field of evolutionary multi-objective optimization (EMO), the following m -objective minimization problem with n decision variables is usually addressed:

$$\text{Minimize } \mathbf{f}(\mathbf{x}) = (f_1(\mathbf{x}), \dots, f_m(\mathbf{x})) \text{ subject to } \mathbf{x} \in X, \quad (1)$$

where $\mathbf{x} = (x_1, x_2, \dots, x_n)$ is an n -dimensional decision vector, $f_i(\mathbf{x})$ is the i th objective to be minimized ($i = 1, 2, \dots, m$), and X is the feasible region. The optimality of solutions is defined by Pareto dominance relation: solution \mathbf{x}^A is referred to as being dominated by solution \mathbf{x}^B if and only if $f_i(\mathbf{x}^B) \leq f_i(\mathbf{x}^A)$ for all i ($i = 1, 2, \dots, m$) and $f_j(\mathbf{x}^B) < f_j(\mathbf{x}^A)$ for at least one j (i.e., $f(\mathbf{x}^B) \leq f(\mathbf{x}^A)$ and $f(\mathbf{x}^B) \neq f(\mathbf{x}^A)$). If solution \mathbf{x}^* is not dominated by any other solutions $\mathbf{x} \in X$, \mathbf{x}^* is a Pareto optimal solution. In other words, a Pareto optimal solution is a non-dominated solution among all feasible solutions $\mathbf{x} \in X$. A non-dominated solution can be defined for any solution set, which is usually a small subset of all feasible solutions (e.g., a population in an EMO algorithm). Pareto optimal solutions are always defined among all feasible solutions $\mathbf{x} \in X$.

The set of all Pareto optimal solutions \mathbf{x}^* is the Pareto set, and the set of objective vectors $\mathbf{f}(\mathbf{x}^*)$ corresponding to all Pareto optimal solutions \mathbf{x}^* is the Pareto front. The number of decision variables n is usually larger than the number of objectives m (i.e., $m < n$) in almost all frequently-used multi-objective test problems such as DTLZ [1] and WFG [2]. In those test problems (except for special

test problems with degenerate Pareto fronts such as the three-objective DTLZ5 and DTLZ6 [3], [4]), the dimensionality of the Pareto set is usually the same as the dimensionality of the Pareto front, which is $(m-1)$. As a result, the mapping from the Pareto set in the n -dimensional decision space to the Pareto front in the m -dimensional objective space is usually a one-to-one mapping as illustrated in Figure 1. Recently, this characteristic feature has been utilized in inverse model-based algorithms [5], [6] and Pareto set learning algorithms [7], [8]. In these algorithms, an inverse model from the Pareto front to the Pareto set is trained using machine learning techniques.

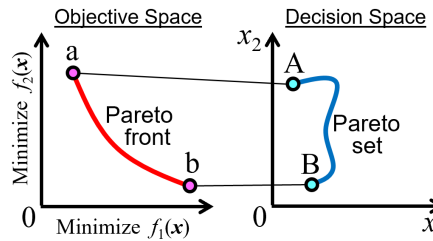


Figure 1: A standard multi-objective problem with a one-to-one mapping between the Pareto set and the Pareto front.

A large number of EMO algorithms have been proposed in the last three decades (e.g., NSGA-II [9], SMS-EMOA [10, 11], MOEA/D [12], NSGA-III [13]). Those algorithms search for a pre-specified number of well-distributed non-dominated solutions to approximate the entire Pareto front. In most EMO algorithms, diversity maintenance of solutions is performed in the objective space. Usually, there is no explicit diversification mechanism in the decision space.

Multi-modal multi-objective optimization [14], [15] is a hot research topic, which is characterized by a one-to-many mapping from the Pareto front to the Pareto set as shown in Figure 2 where each point on the Pareto front corresponds to two points on the Pareto set. Most test problems in frequently-used benchmarking suites (e.g., Omni-test [16], SYM-PART [17], MMF1-15 [18] and MMMOP1-6 [19]) have multiple equivalent Pareto sets. As shown by PS1 and PS2 in Figure 2, each equivalent Pareto set corresponds to the entire Pareto front. Multi-modal multi-objective algorithms usually try to find all of those equivalent Pareto sets.

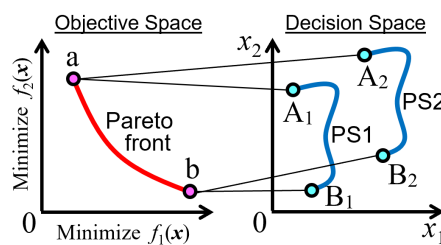


Figure 2: A multi-modal multi-objective problem with two equivalent Pareto sets PS1 and PS2.

The main difficulty in multi-modal multi-objective optimization is to find a good convergence-diversity balance in the decision

space. Since the number of equivalent Pareto sets and their locations are unknown, we need to maintain a large diversity of solutions in the decision space. However, strong diversification often severely degrades the convergence ability. Since early studies in the 2000s [16], [17], a number of multi-modal multi-objective algorithms have been proposed in the EMO community (e.g., [18]-[29]). Those algorithms are designed to find all equivalent Pareto sets. For this purpose, each algorithm has a special diversification mechanism in the decision space. Since the number of equivalent Pareto sets is usually small (typically, two, three or four) in frequently-used multi-modal multi-objective test problems such as MMF1-15 [18] and MMMOP1-6 [19], we can usually obtain well-distributed solutions on both the Pareto front and the Pareto set. That is, in most test problems, there is no strong conflict between the decision space diversity and the objective space diversity (whereas there exists a clear tradeoff relation between the decision space diversification and the decision space convergence). As a result, the main focus in the design of multi-modal multi-objective algorithms is usually placed on how to find a good convergence-diversification balance in the decision space [22].

In real-world application scenarios, it is not likely that there exist equivalent Pareto sets. In other words, it is not likely that the number of corresponding Pareto optimal solutions to each point on the Pareto front is exactly the same. A more realistic scenario is as follows: Each point on the Pareto front corresponds to a different number of Pareto optimal solutions. Motivated by these discussions, in this paper, we propose the use of distance minimization problems based on Manhattan distance as multi-modal multi-objective test problems. An example of our test problems is shown in Figure 3 where the first and second objectives are the minimization of the Manhattan distance from target points A at (15, 15) and B at (5, 5), respectively.

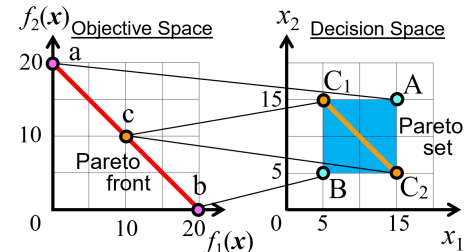


Figure 3: A two-objective distance minimization problem based on Manhattan distance. The first objective is the Manhattan distance from target point A (15, 15), and the second objective is the Manhattan distance from target point B (5, 5).

In Figure 3, the Pareto set is the blue square $[5, 15] \times [5, 15]$, and the Pareto front is the red line. All solutions on the line C_1C_2 are mapped to the midpoint ‘‘c’’ at $(10, 10)$ of the Pareto front since Manhattan distance is used. However, a single point A at $(15, 15)$ in the Pareto set is mapped to a single edge point ‘‘a’’ at $(0, 20)$ of the Pareto front. That is, each point on the Pareto front corresponds to a subset of the Pareto set with a different size.

One clear challenge in our test problem in Figure 3 is that the diversity improvement in the Pareto set does not always lead to the

diversity improvement on the Pareto front. For example, if we randomly sample a pre-specified number of solutions in the Pareto set (i.e., in the blue square in Figure 3), many solutions are obtained around the center of the Pareto front. In this paper, we generalize the decision space from the two-dimensional space in Figure 3 to an n -dimensional space. Then, we explain that we can arbitrarily specify the dimensionality of the Pareto set in an n -dimensional decision space in $\{1, 2, \dots, n\}$. For example, in Figure 3, the dimensionality of the Pareto set is 2. By locating the two target points A and B at $(15, 15)$ and $(5, 15)$, we can create a two-objective problem with the Pareto set on the line AB since the x_2 values of A and B are the same. This idea can be used for the case of $n > 2$. For example, if the two target points A and B are at $(1, 1, 1)$ and $(2, 2, 2)$, the Pareto set is the unit cube between $(1, 1, 1)$ and $(2, 2, 2)$. That is, the dimensionality of the Pareto set is 3. However, if A is at $(1, 1, 1)$ and B is at $(2, 1, 1)$, the Pareto set is the line AB between the two target points A and B. Through computational experiments using some standard EMO algorithms and multi-modal EMO algorithms, we demonstrate that various test problems with different difficulties can be created by changing the number of the decision variables and the locations of the two target points.

This paper is organized as follows. First, in Section 2, we briefly review standard distance minimization problems with Euclidean distance. Next, in Section 3, we explain our two-objective distance minimization problems with Manhattan distance where we show the relation between the locations of the two target points and the dimensionality of the Pareto set. We also discuss the generalization of our two-objective test problems to the following two cases: one is two-objective problems with multiple equivalent Pareto sets, and the other is multi-objective problems with more than two objectives. In Section 4, we formulate a wide variety of test problems with different difficulties by using various settings of the decision space and the target points. Through computational experiments, we demonstrate the difficulties of each problem for standard EMO algorithms and multi-modal EMO algorithms. Finally, we conclude this paper in Section 5.

2 Distance Minimization Problems with Euclidean Distance

In this section, we briefly review distance minimization problems with Euclidean distance. Whereas they are conceptually simple, they have been still actively studied (e.g., see recent papers on problem creation [30] and benchmarking [31]).

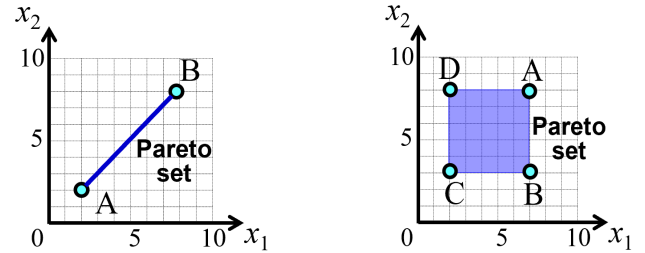
2.1 Multi-Objective Test Problems

Distance minimization problems were first used in the EMO community as many-objective problems in the 2000s [32], [33] to visually examine the search behavior of each EMO algorithm in the two-dimensional decision space. Each objective is the Euclidean distance from the corresponding target point. In Figure 4, we show two examples of distance minimization problems: a two-objective problem in Figure 4 (a) and a four-objective problem in Figure 4 (b). The Pareto set of the two-objective problem is the blue line AB, and the four-objective problem has the square Pareto set ABCD.

Each objective in the two-objective problem in Figure 4 (a) is the distance from the corresponding target point, which is written as

$$f_1(\mathbf{x}) = \text{dist}(\mathbf{x}, A), \quad \text{and} \quad f_2(\mathbf{x}) = \text{dist}(\mathbf{x}, B), \quad (2)$$

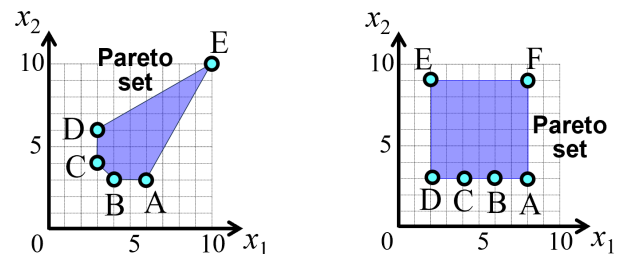
where $\text{dist}(\mathbf{x}, A)$ is the Euclidean distance from the decision vector $\mathbf{x} = (x_1, x_2)$ to point A in the decision space. If we use Manhattan distance, the Pareto set in Fig. 4 (a) is the square specified by the two target points A and B as explained in the next section. The four objectives in Figure 4 (b) are defined as the distance of each target point in the same manner as Eq. (2).



(a) Two-objective problem. (b) Four-objective problem.

Figure 4: Typical distance minimization problems in a two-dimensional decision space.

Distance minimization problems in a two-dimensional decision space have at least two advantages: (i) all solutions in the current population of an EMO algorithm can be easily visualized in the decision space even when their visualization is difficult in a high-dimensional objective space, and (ii) the number of objectives can be easily increased by increasing the number of target points. Actually, the number of objectives was increased up to 15 objectives in [32] and 20 objectives in [33]. By changing the location of each target point, we can easily create test problems with heavily correlated objectives (e.g., using closely located target points A, B, C, D in Figure 5 (a)) and test problems with redundant objectives (e.g., using target points B and C between two target points A and D in Figure 5 (b)). Moreover, by changing the scale of each axis, we can also examine the necessity of normalization. For example, the objective space can be changed from $[0, 10] \times [0, 10]$ to $[0, 0.001] \times [0, 0.001]$, $[0, 1000] \times [0, 1000]$, and $[0, 0.001] \times [0, 1000]$. These special test problems were used to examine the search behavior of EMO algorithms in [34]. Distance minimization problems from multiple target lines were also examined [35].



(a) Correlated objectives. (b) Redundant objectives.

Figure 5: Special distance minimization problems.

The number of decision variables can be easily increased by locating target points in a high-dimensional decision space. Such a high-dimensional distance minimization problem was used in the 2010s to examine the search ability of EMO algorithms for many-objective problems with many decision variables [36], [37].

2.2 Multi-Modal Multi-Objective Test Problems

Multi-modal multi-objective distance minimization problems can be created by locating multiple polygons with enough distance between them [39]. An example with two equivalent Pareto sets is shown in Figure 6 (a) where each objective is defined as

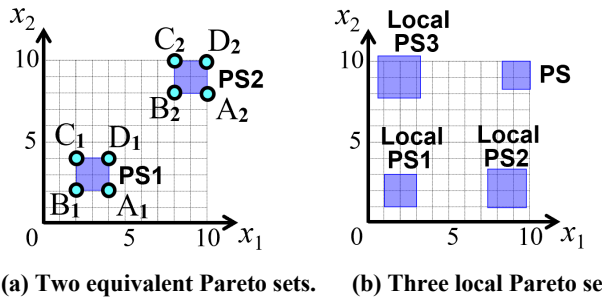
$$f_1(\mathbf{x}) = \text{Min}\{\text{dist}(\mathbf{x}, A_1), \text{dist}(\mathbf{x}, A_2)\}, \quad (3)$$

$$f_2(\mathbf{x}) = \text{Min}\{\text{dist}(\mathbf{x}, B_1), \text{dist}(\mathbf{x}, B_2)\}, \quad (4)$$

$$f_3(\mathbf{x}) = \text{Min}\{\text{dist}(\mathbf{x}, C_1), \text{dist}(\mathbf{x}, C_2)\}, \quad (5)$$

$$f_4(\mathbf{x}) = \text{Min}\{\text{dist}(\mathbf{x}, D_1), \text{dist}(\mathbf{x}, D_2)\}. \quad (6)$$

The SYM-PART problem [17] can be viewed as a multi-modal two-objective distance minimization problem. Multi-modal many-objective problems were used to examine the search behavior of EMO algorithms in the 2010s (e.g., [38]). By using multiple polygons with different sizes as shown in Figure 6 (b), multi-modal many-objective problems with multiple local Pareto sets were also examined in the 2010s (e.g., [39]). In Figure 6 (b), three polygons are local Pareto sets (Local PS1-3).



(a) Two equivalent Pareto sets. (b) Three local Pareto sets.

Figure 6: Multi-modal distance minimization problems.

3 Distance Minimization Problems with Manhattan Distance

In this section, we explain distance minimization problems based on Manhattan distance. Those problems were used to examine the search behavior of EMO algorithms in 2015 [40], [41]. A special setting is the use of a discrete decision space where feasible solutions are defined by integers (e.g., see [42]). In these previous studies, two-dimensional decision spaces were used. In this paper, we use an n -dimensional decision space (e.g., $n = 50$).

3.1 Basic Two-Objective Formulation

Except for the use of Manhattan distance instead of Euclidean distance, the formulation of distance minimization problems based on Manhattan distance is the same as the standard formulation in Section 2. For example, a two-objective problem with target points A and B can be written as follows:

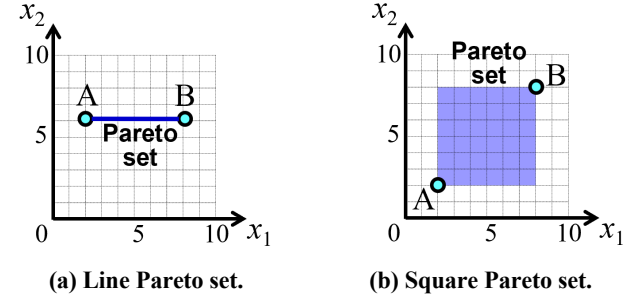
$$\text{Minimize } f_1(\mathbf{x}) = \text{Mdist}(\mathbf{x}, A), \quad (7)$$

$$\text{Minimize } f_2(\mathbf{x}) = \text{Mdist}(\mathbf{x}, B), \quad (8)$$

where $\text{Mdist}(\mathbf{x}, A)$ is the Manhattan distance from solution \mathbf{x} to target point A.

Examples of two-objective Manhattan distance minimization problems are shown in Figure 7. The Pareto set is the blue line in Figure 7 (a), and the blue square in Figure 7 (b). As shown in this figure, the dimensionality of the Pareto set of a two-objective Manhattan distance minimization problem depends on the locations of two target points A and B. In general, let us consider an n -dimensional decision space and two target points $A = (a_1, a_2, \dots, a_n)$ and $B = (b_1, b_2, \dots, b_n)$ where $a_i \leq b_i$ for $i = 1, 2, \dots, n$. If $a_i \neq b_i$ (i.e., $a_i < b_i$ for all i ($i = 1, 2, \dots, n$)), the Pareto set is the n -dimensional hyper-rectangle between A and B: $[a_1, b_1] \times [a_2, b_2] \times \dots \times [a_n, b_n]$. If $a_j = b_j$ for some j , the dimensionality of the Pareto set is decreased. For example, if $a_j = b_j$ for $j = 3, 4, \dots, n$ (i.e., $a_1 \neq b_1$ and $a_2 \neq b_2$), the dimensionality of the Pareto set is 2. In Figure 7 (a), $a_1 \neq b_1$ but $a_2 = b_2$. Thus, the dimensionality of the Pareto set is 1. In this manner, we can arbitrarily specify the dimensionality of the Pareto set as an integer from 1 to n in an n -dimensional decision space.

In some studies (e.g., [41]), Manhattan distance minimization problems were examined in a discrete two-dimensional objective space. If feasible solutions are only at grid points in Figure 7 (b), the midpoint (6, 6) on the Pareto front is mapped from seven Pareto optimal solutions (2, 8), (3, 7), (4, 6), (5, 5), (6, 4), (7, 3) and (8, 2) whereas the edge point (0, 12) is mapped from only one Pareto optimal solution (2, 2), i.e., point A.



(a) Line Pareto set. (b) Square Pareto set.

Figure 7: Manhattan distance minimization problems.

3.2 Formulation with Equivalent Pareto Sets

In the same manner as the standard distance minimization problems (e.g., Figure 6 (a) and (b)), we can create multiple equivalent Pareto sets and local Pareto sets. For example, we have the same two equivalent Pareto sets as in Figure 6 (a) by the following two pairs of target Points: $A_1 = (2, 2)$ and $B_1 = (4, 4)$, and $A_2 = (8, 8)$ and $B_2 = (10, 10)$. In this case, the two objectives are written as follows:

$$f_1(\mathbf{x}) = \text{Min}\{\text{Mdist}(\mathbf{x}, A_1), \text{Mdist}(\mathbf{x}, A_2)\}, \quad (9)$$

$$f_2(\mathbf{x}) = \text{Min}\{\text{Mdist}(\mathbf{x}, B_1), \text{Mdist}(\mathbf{x}, B_2)\}. \quad (10)$$

3.3 Formulation with More Than Two Objectives

Three-objective Manhattan distance minimization problems with three target points were examined in [40] in a two-dimensional

decision space. Then, those problems were extended to the case of many objectives with many target points in [41].

If compared with the standard distance minimization problems, the Pareto set of a multi-objective Manhattan distance minimization problem is much more complicated (see [40], [41]). Figure 8 shows two examples of three-objective Manhattan distance minimization problems. In Figure 8 (a), the Pareto set consists of two lines: AC and BC. In this case, the mapping from the Pareto set to the Pareto front is a one-to-one mapping. In Figure 8 (b), the Pareto set consists of two lines and one square. On each line, the mapping from the Pareto set to the Pareto front is a one-to-one mapping. However, in the square part of the Pareto set, the mapping is many-to-one. As shown in Figure 8, multi-objective Manhattan distance minimization problems are interesting problems. However, at the same time, the identification of the Pareto set is not easy especially in a high-dimensional decision space. For this reason, we use only two-objective Manhattan distance minimization problems in this paper. The use of multi- and many-objective Manhattan distance minimization problem is an interesting future research topic.

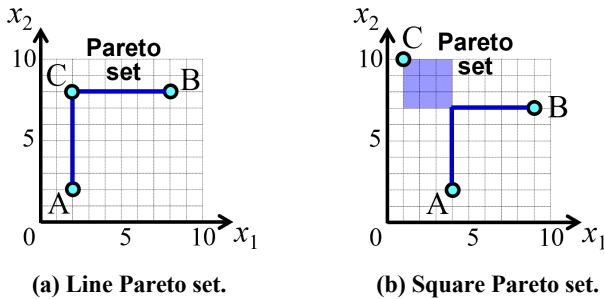


Figure 8: Three-objective Manhattan distance minimization problems with different Pareto set dimensionality.

4 Computational Experiments

In this section, we demonstrate that a wide variety of test problems with different difficulties can be easily created by locating two target points in two- and high-dimensional decision spaces. All test problems are created in continuous decision spaces so that standard EMO and multi-modal EMO algorithms can be used.

4.1 Test Problems

In computational experiments, we create 12 Manhattan distance minimization problems (MDMP1-12) in Table 1. MDMP1 is the basic test problem with two target points A (1, 1) and B (3, 3) in the two-dimensional decision space $[0, 10]^2$. The Pareto set is $[1, 3] \times [1, 3]$. This problem is to examine the distribution of solutions of each algorithm in the two-dimensional Pareto set. MDMP2 has a large decision space $[0, 10000]^2$ to examine the convergence ability of each algorithm. MDMP3 has four equivalent Pareto sets to examine the diversification ability of each algorithm to find all equivalent Pareto sets. MDMP4 has a 10-dimensional decision space $[0, 10]^{10}$. This problem has the same target points as in MDMP1 on the x_1 - x_2 plane. MDMP1 and MDMP4 have the same two-dimensional Pareto set. MDMP4 is to examine the search

ability of each algorithm in a high-dimensional decision space. MDMP5 in $[0, 10]^{20}$ and MDMP6 in $[0, 10]^{50}$ also have the same two-dimensional Pareto set. These problems are to further examine the search algorithm of each algorithm in higher-dimensional decision spaces. MDMP7 has the three-dimensional Pareto set $[1, 3] \times [1, 3] \times [1, 3]$ in the three-dimensional decision space $[0, 10]^3$. This problem is to examine the distribution of solutions in each algorithm in the three-dimensional Pareto set. MDMP8-10 have the same three-dimensional Pareto set in the x_1 - x_2 - x_3 subspace as in MDMP7. These problems are to examine the search ability of each algorithm in higher-dimensional decision spaces: $[0, 10]^{10}$, $[0, 10]^{20}$, and $[0, 10]^{50}$. MDMP11 has the seven-dimensional Pareto set $[1, 3]^7$ in the seven-dimensional decision space $[0, 10]^7$. This problem is to examine the distribution of solutions in the seven-dimensional Pareto set. MDMP12 has two equivalent seven-dimensional Pareto sets to examine whether each algorithm can maintain the diversity of solutions to find the two equivalent Pareto sets.

Table 1: Test problems in this paper: MDMP1-12.

Problem	M	n	Target Points	Space
MDMP1	2	2	A (1, 1), B (3, 3)	$[0, 10]^2$
MDMP2	2	2	Same as MDMP1	$[0, 10000]^2$
MDMP3	2	2	A ₁ (1, 1), B ₁ (3, 3) A ₂ (7, 1), B ₂ (9, 3) A ₃ (1, 7), B ₃ (3, 9) A ₄ (7, 7), B ₄ (9, 9)	$[0, 10]^2$
MDMP4	2	10	A (1, 1, 0, ..., 0) B (3, 3, 0, ..., 0)	$[0, 10]^{10}$
MDMP5	2	20	Same as MDMP4	$[0, 10]^{20}$
MDMP6	2	50	Same as MDMP4	$[0, 10]^{50}$
MDMP7	2	3	A (1, 1, 1), B (3, 3, 3)	$[0, 10]^3$
MDMP8	2	10	A (1, 1, 1, 0, ..., 0) B (3, 3, 3, 0, ..., 0)	$[0, 10]^{10}$
MDMP9	2	20	Same as MDMP8	$[0, 10]^{20}$
MDMP10	2	50	Same as MDMP8	$[0, 10]^{50}$
MDMP11	2	7	A (1, 1, 1, 1, 1, 1, 1) B (3, 3, 3, 3, 3, 3, 3)	$[0, 10]^7$
MDMP12	2	7	A ₁ (1, 1, 1, 1, 1, 1, 1) B ₁ (3, 3, 3, 3, 3, 3, 3) A ₂ (7, 7, 7, 7, 7, 7, 7) B ₂ (9, 9, 9, 9, 9, 9, 9)	$[0, 10]^7$

4.2 Algorithms and Parameter Settings

We apply the following seven algorithms to our 12 test problems: NSGA-II [9], SMS-EMOA [10], [11], MOEA/D-PBI with $\theta = 5$ [12], DN-NSGA-II [20], MMEA-WI [23], HREA [24], and Omni-Optimizer [16]. The first three are well-known and frequently-used EMO algorithms. They are representatives from dominance-based, indicator-based, and decomposition-based algorithms, respectively. The other four are multi-modal EMO algorithms. DN-NSGA-II [20] was proposed in 2016 by including a decision space diversification mechanism. This is one of the earliest multi-modal EMO algorithms. MMEA-WI [23] proposed in 2021 has strong

convergence ability based on a weighted indicator approach. We choose this algorithm as a representative multi-modal EMO algorithm with convergence enhancement. HREA [24] proposed in 2023 has strong diversification ability in the decision space to find not only the Pareto set but also local Pareto sets. We choose this algorithm as a representative multi-modal EMO algorithm with diversification enhancement. We also choose Omni-Optimizer [16] in 2008 as the most well-known multi-modal EMO algorithm.

These seven algorithms are applied to our 12 test problems under the following standard default settings in PlatEMO [43]:

Population size: 100.

Termination condition: 10,000 solution evaluations.

Crossover: SBX crossover with distribution index 20.

Crossover probability: 1.

Mutation: Polynomial mutation with distribution index 20.

Mutation probability: $1/n$.

Number of independent runs: 31.

Experiment Platform: PlatEMO [43].

Among the 31 runs of each algorithm on each test problem, we choose a single run with the median Hypervolume (HV) value of the final population as a representative run to visually show the final population. The reference point for HV calculation is specified as (1.01, 1.01) in the normalized objective space based on the suggestion in [44] for the case of two-objective problems with 100 solutions on linear Pareto fronts. The normalization is performed so that the ideal point is (0, 0) and the nadir point (1, 1) in the normalized objective space. In the original objective space of each algorithm, the true ideal point is (0, 0) since the minimum distance to each target point is always zero, and the true nadir point is calculated by the Manhattan distance between the two target points A and B as ($Mdist(A, B)$, $Mdist(A, B)$). Anytime performance of each algorithm is also shown using the average HV value together with the 95% confidence interval over the 31 runs of each algorithm.

Our goal in this section is to examine the characteristics of our test problems (not to compare the seven algorithms). For rigorous algorithm comparison, we may need to fine-tune parameters for each algorithm (e.g., by automated algorithm configuration [45]) instead of using their default settings.

4.3 Experimental Results

In this section, we show experimental results on each test problem by the three standard EMO algorithms and the four multi-modal EMO algorithms.

MDMP1: The final population of the median HV run of each algorithm on MDMP1 is shown in Figure 9 in the decision space and Figure 10 in the objective space. Since the first three algorithms (in the top row) have no diversification mechanism in the decision space, the obtained solutions are not well distributed in the decision space. Most uniformly distributed solutions in the decision space are obtained by HREA among the examined seven algorithms in Figure 9. However, well distributed solutions in the objective space are not obtained by HREA in Figure 10. This observation suggests the existence of the tradeoff relation between the decision space diversity and the objective space diversity in MDMP1.

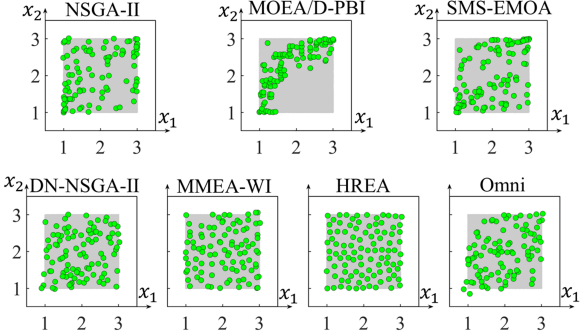


Figure 9: Final population on MDMP1 (Decision Space).

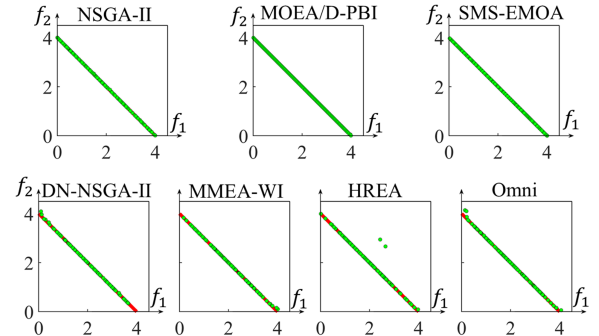


Figure 10: Final population on MDMP1 (Objective Space).

Anytime performance of each algorithm is shown in Figure 11. Since the number of decision variables is only two, and the decision space is small (i.e., $[0, 10] \times [0, 10]$), we cannot observe any clear difference in the convergence speed of each algorithm in Figure 11. In early stage of generations (e.g., before 500 solution examinations), all algorithms show similar improvement curves of the average HV values. After that, the standard EMO algorithms show better performance (i.e., larger average HV values) than the multi-modal EMO algorithms. This is an expected observation since the EMO algorithms focus on the performance only in the objective space.

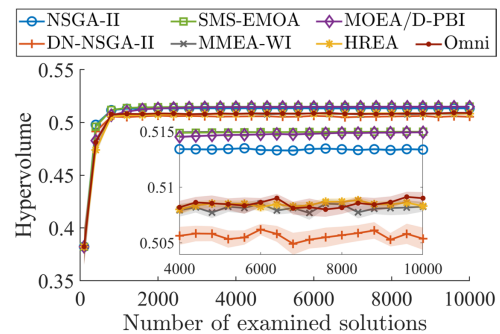


Figure 11: Anytime performance on MDMP1.

MDMP2: By increasing the decision space size from $[0, 10]^2$ in MDMP1 to $[0, 10000]^2$ in MDMP2, the convergence difficulty is increased in MDMP2. The anytime performance of each algorithm

in MDMP2 is shown in Figure 12. We can observe the clearly slow convergence of HREA with the strong diversification mechanism in the decision space. In Figure 12, MOEA/D-PBI and MMEA-WI also show weaker anytime performance than the other algorithms.

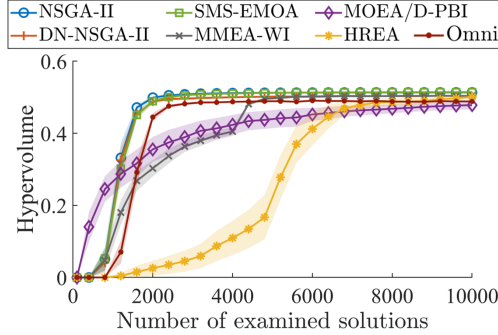


Figure 12: Anytime performance on MDMP2.

MDMP3: This problem has four equivalent Pareto sets. The final population of each algorithm is shown in Figure 13 in the decision space and Figure 14 in the objective space.

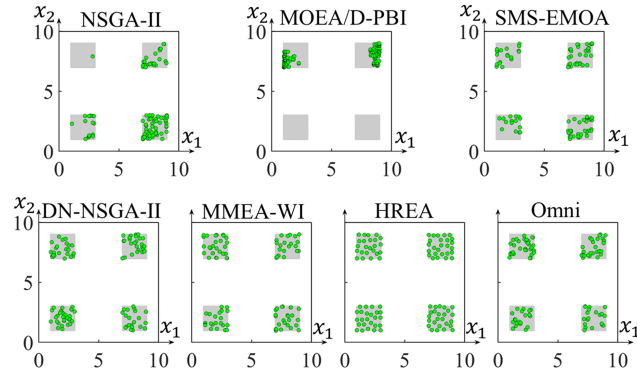


Figure 13: Final population on MDMP3 (Decision Space).

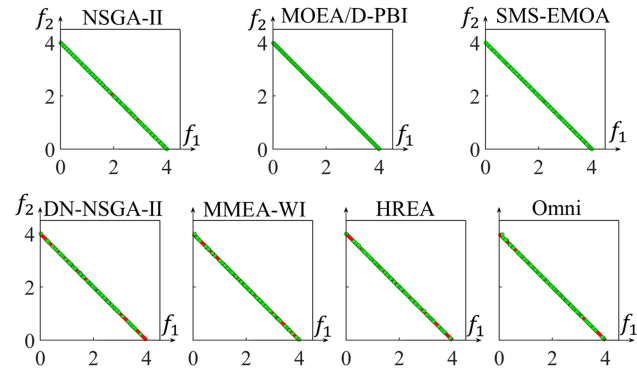


Figure 14: Final population on MDMP3 (Objective Space).

All the four multi-modal EMO algorithms find all the four equivalent Pareto sets. The most uniformly distributed solutions in the decision space in Figure 13 are obtained by HREA as in the case

of MDMP1 in Figure 9. The solution distributions in the objective space by the four multi-modal EMO algorithms in Figure 14 are not good if compared with the three EMO algorithms.

MDMP4-6: MDMP4-6 are basically the same problems with a different number of decision variables (i.e., different specifications of n). As shown in Figures 15-17, the increase in the number of decision variables (i.e., the increase of n) increases the convergence difficulty of the problem.

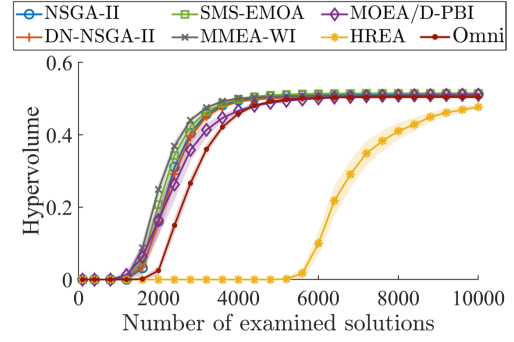


Figure 15: Anytime performance on MDMP4 ($n = 10$).

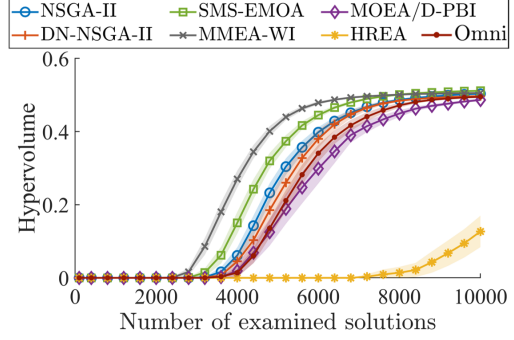


Figure 16: Anytime performance on MDMP5 ($n = 20$).

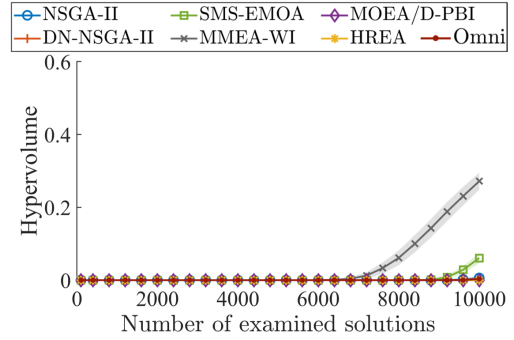


Figure 17: Anytime performance on MDMP6 ($n = 50$).

As expected from the previous results (e.g., Figure 12), HREA shows the slowest convergence in Figures 15 and 16. One interesting observation is that MMEA-WI shows the strongest convergence ability in Figures 16 and 17 whereas it is a multi-modal EMO algorithm.

MDMP7: MDMP7 has the three-dimensional Pareto set $[1, 3]^3$ in the three-dimensional decision space $[0, 10]^3$. The final population of each algorithm is shown in Figure 18 in the decision space and Figure 19 in the objective space. In Figure 18, the final populations of MMEA-WI and HREA have good distributions in the decision space. However, their distributions in the objective space are not good (e.g., solutions are sparse around $(0, 6)$ and $(6, 0)$). These observations show that our Manhattan distance minimization problems have a clear tradeoff between the decision space uniformity and the objective space uniformity.

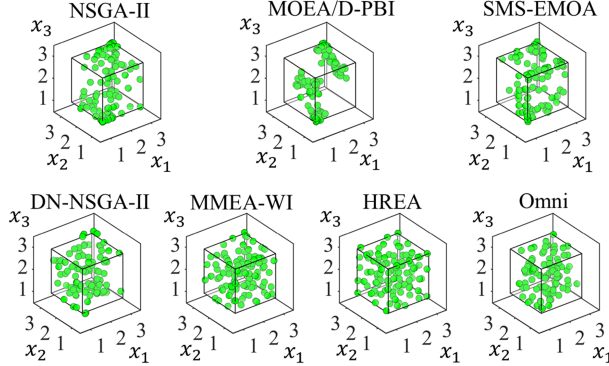


Figure 18: Final population on MDMP7 (Decision Space).

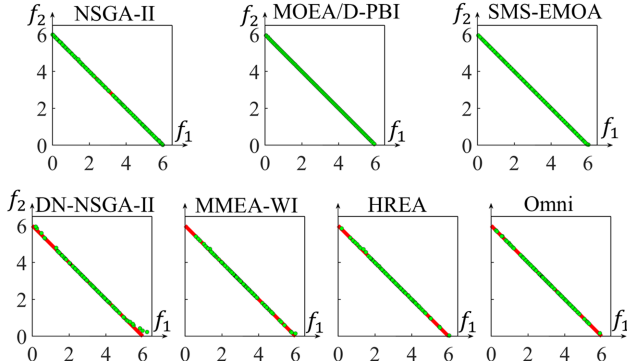


Figure 19: Final population on MDMP7 (Objective Space).

MDMP8-10: These problems are basically the same problems as MDMP7 with a different number of decision variables. The same three-dimensional Pareto set is placed in the decision spaces with a different dimensionality: $[0, 10]^{10}$ in MDMP8, $[0, 10]^{20}$ in MDMP9, and $[0, 10]^{50}$ in MDMP10. As we have already shown in Figures 15-17, it is expected that the increase in the number of decision variables (i.e., the increase of n) will make our test problems more difficult. Anytime performance of each algorithm on each test problem is shown in Figures 20-22. As expected, we can observe clear performance deterioration by increasing the number of decision variables from 10 to 50 in Figures 20-22. The strongest convergence is obtained by the convergence enhanced multi-modal EMO algorithm MMEA-WI, and the weakest convergence ability is obtained by the diversity enhanced multi-modal EMO algorithm HREA. From the comparison between Figures 15-17 with the two-

dimensional Pareto set and Figure 20-22 with the three-dimensional Pareto set, we can see that the dimensionality of the decision space has much larger effects than the dimensionality of the Pareto set on the convergence ability of each algorithm.

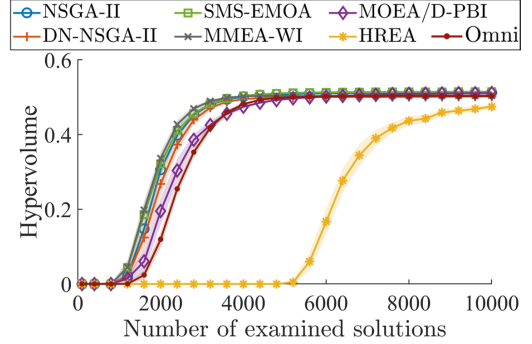


Figure 20: Anytime performance on MDMP8 ($n = 10$).

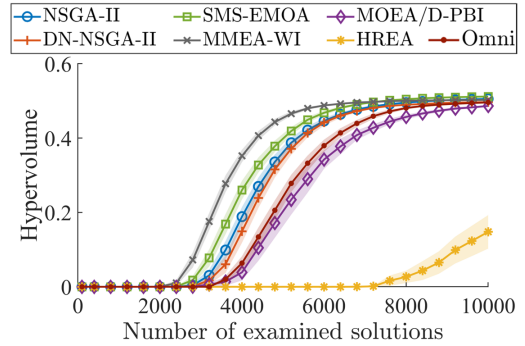


Figure 21: Anytime performance on MDMP9 ($n = 20$).

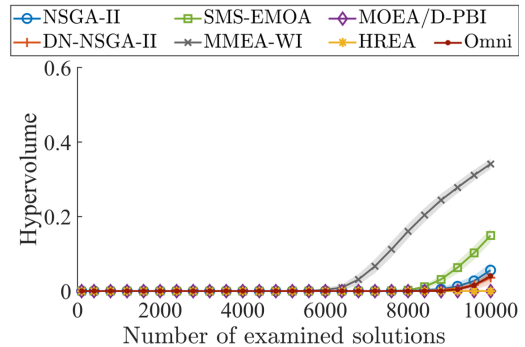


Figure 22: Anytime performance on MDMP10 ($n = 50$).

MDMP11: This test problem has the seven-dimensional Pareto set $[1, 3]^7$ in the seven-dimensional decision space $[0, 10]^7$. Experimental results are shown in Figures 23-25.

In Figure 24, the final population of each algorithm in the seven-dimensional decision space is shown in the x_1 - x_2 subspace (i.e., the x_1 - x_2 plane projection). Except for HREA, the final population of each algorithm has converged to the Pareto front in Figure 25 (and the Pareto set in Figure 24). This means that the increase in the

dimensionality of the Pareto set does not severely degrade the performance of each algorithm (except for HREA). However, it clearly increases the difficulty for the multi-modal EMO algorithms to find well-distributed solutions in the objective space in Figure 25. No solutions are obtained around the two edges of the Pareto front (i.e., (0, 14) and (14, 0)) by the multi-modal EMO algorithms.

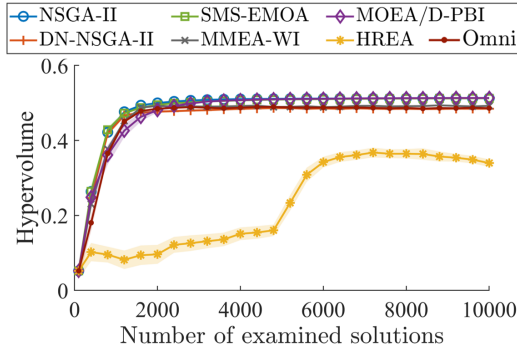


Figure 23: Anytime performance on MDMP11 ($n = 7$).

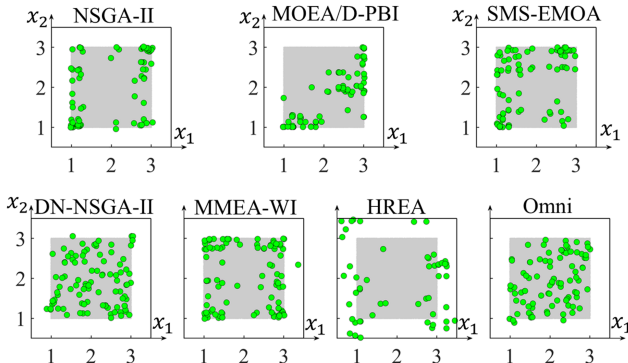


Figure 24: Final population on MDMP11 (projections on the x_1 - x_2 plane in the seven-dimensional decision space).

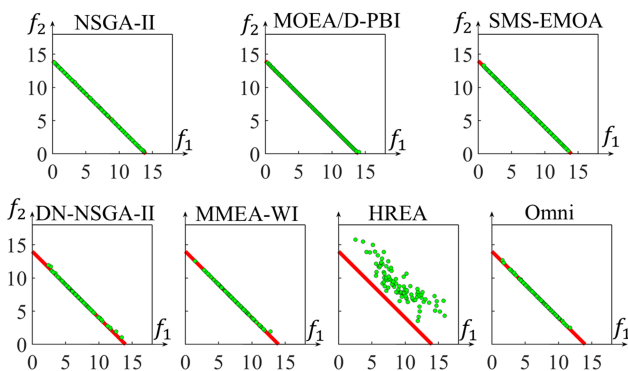


Figure 25: Final population on MDMP11 (Objective Space).

MDMP12: This problem has two equivalent seven-dimensional Pareto sets. Experimental results are shown in Figures 26-28.

In Figure 26, the convergence is not difficult except for HREA. However, it is difficult to find the two equivalent Pareto sets for the

standard EMO algorithm in Figure 27. Moreover, it is difficult for the multi-modal EMO algorithms to find well-distributed solutions over the entire Pareto front in Figure 28. No solutions around the two edges of the Pareto front are obtained by the multi-modal EMO algorithms. This observation (and the similar observation in Figure 25) suggests the existence of the tradeoff relation between decision space diversity and objective space diversity.

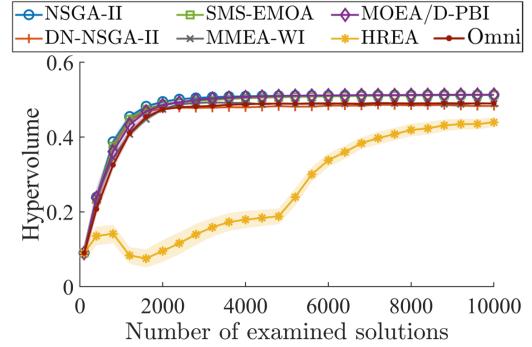


Figure 26: Anytime performance on MDMP12 ($n = 7$).

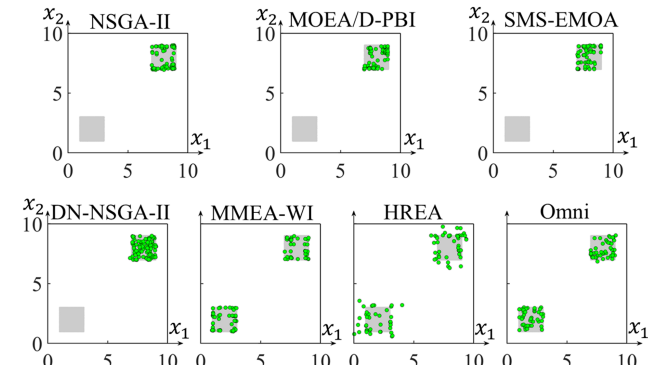


Figure 27: Final population on MDMP12 (projections on the x_1 - x_2 plane in the seven-dimensional decision space).

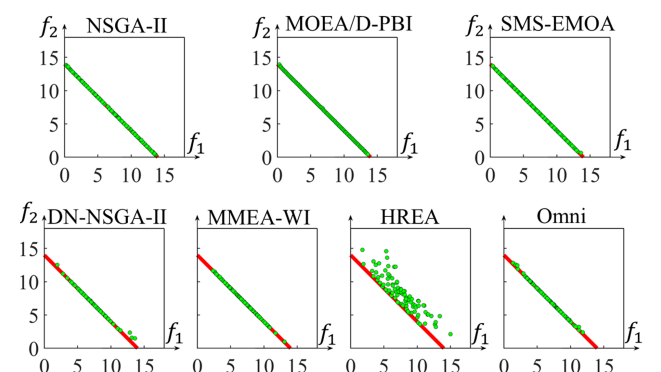


Figure 28: Final population on MDMP12 (Objective Space).

Our experimental results clearly showed that HREA has strong diversification ability in the decision space and weak convergence ability in the objective space. To further examine its convergence

ability in the objective space, we perform the same experiments on MDMP12 using ten times larger computational budget. That is, we increase the number of examined solutions in each algorithm from 10,000 to 100,000. Anytime performance of each algorithm is shown in Figure 29. Since HREA has a strong diversification mechanism in the decision space, the convergence of solutions in the objective space is still weak even after a large number of generation updates in Figure 29.

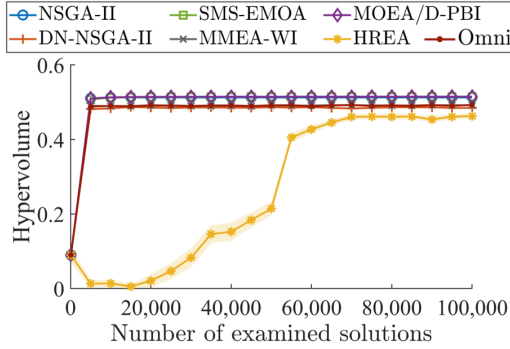


Figure 29: Anytime performance on MDMP12 ($n = 7$). The termination condition is 100,000 solution evaluations in Figure 29 whereas it is 10,000 solution evaluations in Figure 26.

To examine the effects of using Manhattan distance instead of Euclidean distance in distance minimization problems, we perform computational experiments on our MDMP1-12 test problems using Euclidean distance. Some experimental results are shown below.

MDMP3 with Euclidean Distance: The final population of each algorithm is shown in Figure 30 in the decision space and Figure 31 in the objective space.

In Figure 30, each algorithm shows different diversification ability in the decision space. However, in Figure 31, almost the same results are obtained by all algorithms, which is clearly different from Figure 14. These observations show that the use of Euclidean distance cannot create a clear tradeoff between the decision space diversity and the objective space diversity. That is, the use of Manhattan distance creates the difficulty in objective space diversification together with decision space diversification.

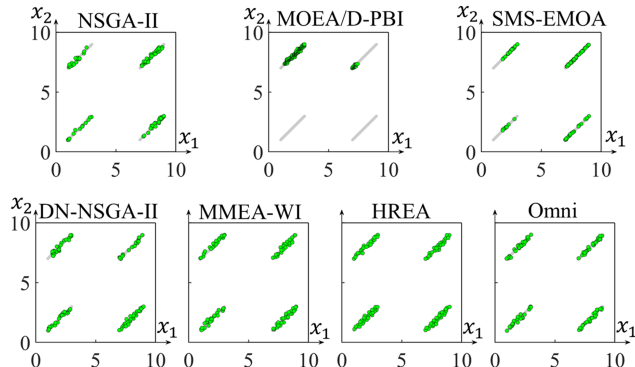


Figure 30: MDMP3 with Euclidean distance (Decision Space).

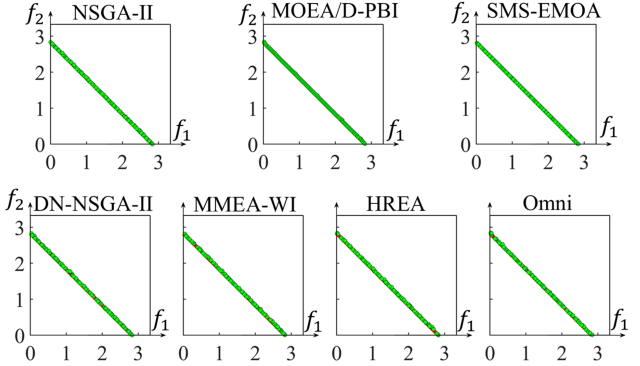


Figure 31: MDMP3 with Euclidean distance (Objective Space).

MDMP4-6 with Euclidean distance: Experimental results are shown in Figures 32-34. As in the case of Manhattan distance in Figure 15-17, the increase in the number of decision variables increases the convergence difficulty in Figures 32-34.

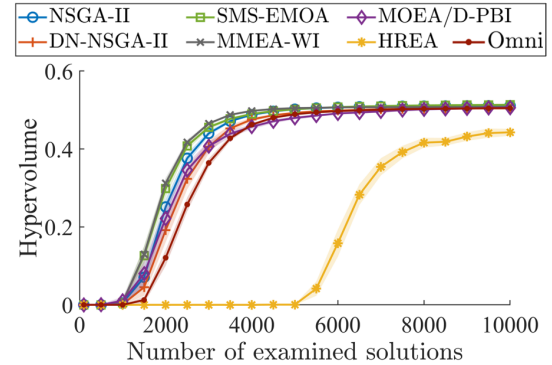


Figure 32: MDMP4 with Euclidean distance ($n = 10$).

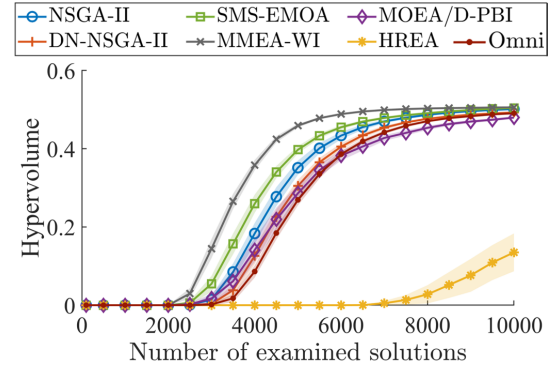


Figure 33: MDMP5 with Euclidean distance ($n = 20$).

These additional experiments in Figures 30-34 show that the use of Manhattan distance in distance minimization problems increases the objective space diversification difficulty (as shown by the comparison between Figure 14 and Figure 31). However, it does not have large effects on the decision space diversification difficulty and the convergence difficulty to the Pareto front.

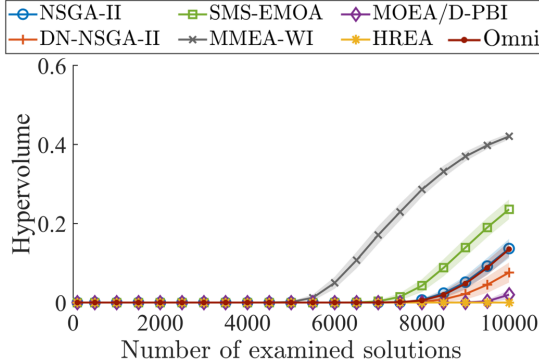


Figure 34: MDMP6 with Euclidean distance ($n = 50$).

5 Conclusions and Future Topics

In this paper, we formulated 12 distance minimization problems based on Manhattan distance. Those problems can be viewed as multi-modal multi-objective test problems with the following two features. (i) One feature is that the number of corresponding Pareto solutions to a single point on the Pareto front is different depending on the location of the point on the Pareto front. A point around the center of the Pareto front has many Pareto optimal solutions, and a point on the edges of the Pareto front has only a single Pareto optimal solution. This is clearly different from the standard multi-modal multi-objective test problems where each point on the Pareto front has the same number of corresponding Pareto optimal solutions (since those problems have multiple equivalent Pareto sets). (ii) The other feature of our test problems is that the dimensionality of the Pareto set can be arbitrarily specified between 1 and n in an n -dimensional decision space. This is also clearly different from the standard multi-modal multi-objective test problems where the dimensionality of the Pareto set is usually $(m-1)$ in m -objective problems. Our test problems include up to 50 decision variables (i.e., $n = 50$) and 2-, 3- and 7-dimensional Pareto sets. The decision space dimensionality and the Pareto set dimensionality can be arbitrarily specified in our test problems.

Using the formulated 12 test problems, we examined the search behavior of three EMO algorithms and four multi-modal EMO algorithms. Our experimental results clearly showed the following two tradeoff relations: (i) the diversity-convergence tradeoff in the decision space, and (ii) the tradeoff relation between decision space diversity and objective space diversity. The first type of tradeoff relation has been frequently discussed in the literature. This tradeoff is almost the same as the frequently-discussed tradeoff relation between decision space diversity and objective space convergence [45]. In our experiments, HREA [24] with strong diversification ability showed the slowest convergence among the examined algorithms. However, the second type of tradeoff relation has not been discussed in many studies on multi-modal multi-objective optimization. This is because the diversification in the decision space usually leads to the diversification in the objective space in most of the standard frequently-used multi-modal multi-objective test problems (e.g., see Figures 30 and 31). Our experiments demonstrated that the good uniformity of solutions

over the entire Pareto set does not mean the good uniformity over the entire Pareto front (e.g., see Figures 18 and 19).

One future research direction is to examine various aspects of multi-modal multi-objective optimization by creating other test problems. Using the same framework as our 12 test problems, we can formulate a wide variety of test problems for examining various aspects of multi-modal multi-objective optimization. Another future research direction is the formulation and the use of many-objective Manhattan distance minimization problems in a high-dimensional decision space. All of our test problems in this paper have only two objectives (i.e., pairs of target points) whereas the number of decision variables and the dimensionality of the Pareto set can be arbitrarily specified. The identification of the Pareto set in a high-dimensional Manhattan distance minimization problem with more than two target points will be an interesting challenge since complicated analysis is needed even for the case of a two-dimensional decision space [40], [41]. Another future research direction is to formulate test problems based on realistic city maps where the distance between two locations is defined by Manhattan distance. In some large cities, Manhattan distance is more realistic than Euclidean distance. In this formulation, the decision space will be a set of discrete points.

For further fruitful advances of the multi-modal multi-objective optimization research field, especially, for the design of practically useful algorithms, good test problems are needed to analyze the search behavior of each algorithm. This paper is one attempt in this direction. For test problem creation, there also exist many other attempts in the literature [46]-[48]. Visualization is also important for algorithm analysis. In this paper, we use simple visualization methods. Our reported results can be more clearly shown by using other visualization methods [49]-[50].

ACKNOWLEDGMENTS

This work was supported by National Natural Science Foundation of China (Grant No. 62376115), the National Key R&D Program of China (Grant No. 2023YFE0106300), Guangdong Provincial Key Laboratory (Grant No.2020B121201001).

REFERENCES

- [1] K. Deb, L. Thiele, M. Laumanns, and E. Zitzler. 2002. Scalable multi-objective optimization test problems. In *Proceedings of 2002 Congress on Evolutionary Computation* (CEC 2002), IEEE, Honolulu, USA, 825-830.
- [2] S. Huband, P. Hingston, L. Barone, and L. While. 2006. A review of multiobjective test problems and a scalable test problem toolkit. *IEEE Trans. on Evolutionary Computation* 10, 5 (2006), 477-506.
- [3] D. K. Saxena, J. A. Duro, A. Tiwari, K. Deb, and Q. Zhang. 2013. Objective reduction in many-objective optimization: Linear and nonlinear algorithms. *IEEE Trans. on Evolutionary Computation* 17, 1 (2013) 77-99.
- [4] H. Ishibuchi, H. Masuda, and Y. Nojima. 2016. Pareto fronts of many-objective degenerate test problems. *IEEE Trans. on Evolutionary Computation* 20, 5 (2016) 807-813.
- [5] R. Cheng, Y. Jin, K. Narukawa, and B. Sendhoff. 2015. A multiobjective evolutionary algorithm using Gaussian process-based inverse modeling. *IEEE Trans. on Evolutionary Computation* 19, 6 (2015) 838-856.
- [6] H. Zhang, J. Ding, M. Jiang, K. C. Tan, and T. Chai. 2021. Inverse Gaussian process modeling for evolutionary dynamic multiobjective optimization. *IEEE Trans. on Cybernetics* 52, 10 (2021) 11240-11253.
- [7] X. Lin, Z. Yang, X. Zhang, and Q. Zhang. 2022. Pareto set learning for expensive multi-objective optimization. In *Proceedings of the 36th Conference of Advances in Neural Information Processing Systems* (NeurIPS 2022), New Orleans, USA, 19231-19247.

- [8] X. Lin, X. Zhang, Z. Yang, F. Liu, Z. Wang, and Q. Zhang. 2024. Smooth Tchebycheff scalarization for multi-objective optimization. In *Proceedings of the 41st International Conference on Machine Learning (ICML 2024)*, Vienna, Austria, 30479-30509.
- [9] K. Deb, A. Pratap, S. Agarwal, and T. Meyarivan. 2002. A fast and elitist multiobjective genetic algorithm: NSGA-II. *IEEE Trans. on Evolutionary Computation* 6, 2 (2002) 182-197.
- [10] M. Emmerich, N. Beume, and B. Naujoks. 2005. An EMO algorithm using the hypervolume measure as selection criterion. In *Proceedings of 3rd International Conference on Evolutionary Multi-Criterion Optimization (EMO 2005)*, Springer, Guanajuato, Mexico, 62-76.
- [11] N. Beume, B. Naujoks, and M. Emmerich. 2007. SMS-EMOA: Multiobjective selection based on dominated hypervolume. *European Journal of Operational Research* 181, 3 (2007), 1653-1669.
- [12] Q. Zhang and H. Li. 2007. MOEA/D: A multiobjective evolutionary algorithm based on decomposition. *IEEE Trans. on Evolutionary Computation* 11, 6 (2007), 712-731.
- [13] K. Deb and H. Jain. 2014. An evolutionary many-objective optimization algorithm using reference-point-based non-dominated sorting approach, Part I: Solving problems with box constraints. *IEEE Trans. on Evolutionary Computation* 18, 4 (2014) 577-601.
- [14] R. Tanabe and H. Ishibuchi. 2020. A review of evolutionary multi-modal multi-objective optimization. *IEEE Trans. on Evolutionary Computation* 24, 1 (2020) 193-200.
- [15] C. Grimme, P. Kerschke, P. Aspar, H. Trautmann, M. Preuss, A. H. Deutz, H. Wang, and M. Emmerich. 2021. Peeking beyond peaks: Challenges and research potentials of continuous multimodal multi-objective optimization. *Computers & Operations Research* 136 (2021) Article 105489.
- [16] K. Deb and S. Tiwari. 2008. Omni-optimizer: A generic evolutionary algorithm for single and multi-objective optimization. *European Journal of Operational Research* 185, 3 (2008) 1062-1087.
- [17] G. Rudolph, B. Naujoks, and M. Preuss. 2007. Capabilities of EMOA to detect and preserve equivalent Pareto subsets. In *Proceedings of 4th International Conference on Evolutionary Multi-Criterion Optimization (EMO 2007)*, Springer, Matsushima, Japan, 36-50.
- [18] C. Yue, B. Qu, K. Yu, J. Liang, and X. Li. 2019. A novel scalable test problem suite for multimodal multiobjective optimization. *Swarm and Evolutionary Computation* 48 (2019) 62-71.
- [19] Y. Liu, G. G. Yen, and D. Gong. 2019. A multimodal multiobjective evolutionary algorithm using two-archive and recombination strategies. *IEEE Trans. on Evolutionary Computation* 23, 4 (2019) 660-674.
- [20] J. J. Liang, C. T. Yue, and B. Y. Qu. 2016. Multimodal multi-objective optimization: A preliminary study. In *Proceedings of 2016 IEEE Congress on Evolutionary Computation (IEEE CEC 2016)*. Vancouver, Canada, 2454-2461.
- [21] C. Yue, B. Qu, J. Liang. 2018. A multiobjective particle swarm optimizer using ring topology for solving multimodal multiobjective problems. *IEEE Trans. on Evolutionary Computation* 22, 5 (2018), 805-817.
- [22] Y. Liu, H. Ishibuchi, G. G. Yen, Y. Nojima, and N. Masuyama. 2020. Handling imbalance between convergence and diversity in the decision space in evolutionary multi-modal multi-objective optimization. *IEEE Trans. on Evolutionary Computation* 24, 3 (2020) 551-565.
- [23] W. Li, T. Zhang, R. Wang, and H. Ishibuchi. 2021. Weighted indicator-based evolutionary algorithm for multimodal multiobjective optimization. *IEEE Trans. on Evolutionary Computation* 25, 6 (2021) 1064-1078.
- [24] W. Li, X. Yao, T. Zhang, R. Wang, and L. Wang. 2023. Hierarchy ranking method for multimodal multiobjective optimization with local Pareto fronts. *IEEE Transactions on Evolutionary Computation* 27, 1 (2023), 98-110.
- [25] S. Long, J. Zheng, Q. Deng, Y. Liu, J. Zou, and S. Yang. 2024. A similarity-detection-based evolutionary algorithm for large-scale multimodal multi-objective optimization. *Swarm and Evolutionary Computation* 87 (2024) Article ID 101548.
- [26] J. Liang, X. Sui, C. Yue, M. Yu, G. Li, and M. Li. 2024. Multimodal multiobjective differential evolution algorithm based on enhanced decision space search. *Swarm and Evolutionary Computation* 90 (2024) Article ID 101682.
- [27] Q. Dang, G. Zhang, L. Wang, Y. Yu, S. Yang, X. He. 2025. Transformer-based intelligent prediction model for multimodal multi-objective optimization. *IEEE Computational Intelligence Magazine* 20, 1 (2025) 34-49.
- [28] Q. Dang, G. Zhang, L. Wang, S. Yang, and T. Zhan. 2024. A generative adversarial networks model based evolutionary algorithm for multimodal multi-objective optimization. *IEEE Transactions on Emerging Topics in Computational Intelligence*. (Early Access Paper).
- [29] Q. Dang, Q. Liu, S. Yang, and X. He. 2025. Data-driven evolutionary algorithm based on inductive graph neural networks for multimodal multi-objective optimization. *IEEE Trans. on Evolutionary Computation*. (Early Access Paper).
- [30] J. E. Fieldsend, T. Chugh, R. Allmendinger, and K. Miettinen. 2022. A visualizable test problem generator for many-objective optimization. *IEEE Trans. on Evolutionary Computation* 26, 1 (2022) 1-11.
- [31] A. Liefoghe, S. Verel, T. Chugh, J. Fieldsend, R. Allmendinger, and K. Miettinen. 2023. Feature-based benchmarking of distance-based multi/many-objective optimisation problems: A machine learning perspective. In *Proceedings of 12th International Conference on Evolutionary Multi-Criterion Optimization (EMO 2023)* Springer, Leiden, Netherlands, 260-273.
- [32] M. Köppen and K. Yoshida. 2007. Substitute distance assignments in NSGA-II for handling many-objective optimization problems. In *Proceedings of 4th International Conference on Evolutionary Multi-Criterion Optimization (EMO 2007)*, Springer, Matsushima, Japan, 727-741.
- [33] H. K. Singh, A. Isaacs, T. Ray, and W. Smith. 2008. A study on the performance of substitute distance based approaches for evolutionary many objective optimization. In *Proceedings of 7th International Conference on Simulated Evolution and Learning (SEAL 2008)*, Springer, Melbourne, Australia, 401-410.
- [34] H. Ishibuchi and L. M. Pang. 2025. Visual explanations of some problematic search behaviors of frequently-used EMO algorithms. In *Proceedings of 13th International Conference on Evolutionary Multi-Criterion Optimization (EMO 2025)* Vol. II, Springer Canberra, Australia, 3-16.
- [35] M. Li, C. Grosan, S. Yang, X. Liu, and X. Yao. 2018. Multiline distance minimization: A visualized many-objective test problem suite. *IEEE Trans. on Evolutionary Computation* 22, 1 (2018) 61-78.
- [36] O. Schutze, A. Lara, and C. A. C. Coello. 2011. On the influence of the number of objectives on the hardness of multiobjective optimization problem. *IEEE Trans. on Evolutionary Computation* 15, 4 (2011) 444-455.
- [37] H. Masuda, Y. Nojima, and H. Ishibuchi. 2014. Visual examination of the behavior of EMO algorithms for many-objective optimization with many decision variables. In *Proceedings of 2014 IEEE Congress on Evolutionary Computation (IEEE CEC 2014)*, IEEE, Beijing, China, 2633-2640.
- [38] H. Ishibuchi, Y. Hitotsuyanagi, N. Tsukamoto, and Y. Nojima. 2010. Many-objective test problems to visually examine the behavior of multiobjective evolution in a decision space. In *Proceedings of 11th International Conference on Parallel Problem Solving from Nature (PPSN 2010)* Part II, Springer, Krakow, Poland, 91-100.
- [39] H. Ishibuchi, Y. Peng, and K. Shang. 2019. A scalable multimodal multiobjective test problem. In *Proceedings of 2019 IEEE Congress on Evolutionary Computation (IEEE CEC 2019)*, IEEE, Wellington, New Zealand, 302-309.
- [40] H. Zille and S. Mostaghim. 2015. Properties of scalable distance minimization problems using the Manhattan metric. In *Proceedings of 2015 IEEE Congress on Evolutionary Computation (IEEE CEC 2015)*, IEEE, Sendai, Japan, 2875-2882.
- [41] J. Xu, K. Deb, and A. Gaur. 2015. Identifying the Pareto-optimal solutions for multi-point distance minimization problem in Manhattan space. *Michigan State University COIN Report* (2015) Report ID: 2015018.
- [42] G. Rudolph and M. Wagner. 2025. Cumulative step size adaptation for adaptive SEMO in integer space. In *Proceedings of 13th International Conference on Evolutionary Multi-Criterion Optimization (EMO 2025)* Vol. I, Springer, Canberra, Australia, 118-131.
- [43] Y. Tian, R. Cheng, X. Zhang, and Y. Jin. 2017. PlatEMO: A MATLAB platform for evolutionary multi-objective optimization. *IEEE Computational Intelligence Magazine* 12, 4 (2017), 73-87.
- [44] H. Ishibuchi, R. Imada, Y. Setoguchi, and Y. Nojima. 2018. How to specify a reference point in hypervolume calculation for fair performance comparison. *Evolutionary Computation* 26, 3 (2018) 411-440.
- [45] O. L. Preuß, J. Rook, and H. Trautmann. 2024. On the potential of multi-objective automated algorithm configuration on multi-modal multi-objective optimisation problems. In *Proceeding of 27th European Conference on Applications of Evolutionary Computation (EvoApplications 2024)*, Springer, Aberystwyth, UK, 305-321.
- [46] T. Glasmachers. 2019. Challenges of convex quadratic bi-objective benchmark problems. In *Proceedings of 2019 Genetic and Evolutionary Computation Conference (GECCO 2019)*, ACM, Prague, Czech Republic, 559-567.
- [47] D. Brockhoff, A. Auger, N. Hansen, and T. Tušar. 2022. Using well-understood single-objective functions in multiobjective black-box optimization test suites. *Evolutionary Computation* 30, 2 (2022), 165-193.
- [48] L. Schäpermeier, P. Kerschke, C. Grimme, and H. Trautmann. 2023. Peak-A-Boo! Generating multi-objective multiple peaks benchmark problems with precise Pareto sets. In *Proceedings of 12th International Conference on Evolutionary Multi-Criterion Optimization (EMO 2023)*, Springer, Leiden, Netherlands, 291-304.
- [49] T. Tušar and B. Filipic. 2015. Visualization of Pareto front approximations in evolutionary multiobjective optimization: A critical review and the prosecution method. *IEEE Trans. on Evolutionary Computation* 19, 2 (2015), 225-245.
- [50] L. Schäpermeier, C. Grimme, and P. Kerschke. 2022. Plotting impossible? Surveying visualization methods for continuous multi-objective benchmark problems. *IEEE Trans. on Evolutionary Computation* 26, 6 (2022), 1306-1320.